

## Interferometry of Direct Photons in Central $^{208}\text{Pb} + ^{208}\text{Pb}$ Collisions at 158A GeV

M. M. Aggarwal,<sup>1</sup> Z. Ahammed,<sup>2</sup> A. L. S. Angelis,<sup>3,\*</sup> V. Antonenko,<sup>4</sup> V. Arefiev,<sup>5</sup> V. Astakhov,<sup>5</sup> V. Avdeitchikov,<sup>5</sup> T. C. Awes,<sup>6</sup> P. V. K. S. Baba,<sup>7</sup> S. K. Badyal,<sup>7</sup> S. Bathe,<sup>8</sup> B. Batiounia,<sup>5</sup> T. Bernier,<sup>9</sup> K. B. Bhalla,<sup>10</sup> V. S. Bhatia,<sup>1</sup> C. Blume,<sup>8</sup> D. Bucher,<sup>8</sup> H. Büsching,<sup>8</sup> L. Carlén,<sup>11</sup> S. Chattopadhyay,<sup>2</sup> M. P. Decowski,<sup>12</sup> H. Delagrange,<sup>9</sup> P. Donni,<sup>3</sup> M. R. Dutta Majumdar,<sup>2</sup> K. El Chenawi,<sup>11</sup> A. K. Dubey,<sup>13</sup> K. Enosawa,<sup>14</sup> S. Fokin,<sup>4</sup> V. Frolov,<sup>5</sup> M. S. Ganti,<sup>2</sup> S. Garpman,<sup>11,\*</sup> O. Gavrishchuk,<sup>5</sup> F. J. M. Geurts,<sup>15</sup> T. K. Ghosh,<sup>16</sup> R. Glasow,<sup>8</sup> B. Guskov,<sup>5</sup> H. Å. Gustafsson,<sup>11</sup> H. H. Gutbrod,<sup>17</sup> I. Hrivnacova,<sup>18</sup> M. Ippolitov,<sup>4</sup> H. Kalechofsky,<sup>3</sup> K. Karadjev,<sup>4</sup> K. Karpio,<sup>19</sup> B. W. Kolb,<sup>17</sup> I. Kosarev,<sup>5</sup> I. Koutcheryaev,<sup>4</sup> A. Kugler,<sup>18</sup> P. Kulinich,<sup>12</sup> M. Kurata,<sup>14</sup> A. Lebedev,<sup>4</sup> H. Löhner,<sup>16</sup> L. Luquin,<sup>9</sup> D. P. Mahapatra,<sup>13</sup> V. Manko,<sup>4</sup> M. Martin,<sup>3</sup> G. Martínez,<sup>9</sup> A. Maximov,<sup>5</sup> Y. Miake,<sup>14</sup> G. C. Mishra,<sup>13</sup> B. Mohanty,<sup>13</sup> M.-J. Mora,<sup>9</sup> D. Morrison,<sup>20</sup> T. Moukhanova,<sup>4</sup> D. S. Mukhopadhyay,<sup>2</sup> H. Naef,<sup>3</sup> B. K. Nandi,<sup>13</sup> S. K. Nayak,<sup>7</sup> T. K. Nayak,<sup>2</sup> A. Nianine,<sup>4</sup> V. Nikitine,<sup>5</sup> S. Nikolaev,<sup>4</sup> P. Nilsson,<sup>11</sup> S. Nishimura,<sup>14</sup> P. Nomokonov,<sup>5</sup> J. Nystrand,<sup>11</sup> A. Oskarsson,<sup>11</sup> I. Otterlund,<sup>11</sup> T. Peitzmann,<sup>15</sup> D. Peressounko,<sup>4</sup> V. Petracek,<sup>18</sup> S. C. Phatak,<sup>13</sup> W. Pinganaud,<sup>9</sup> F. Plasil,<sup>6</sup> M. L. Purschke,<sup>17</sup> J. Rak,<sup>18</sup> R. Raniwala,<sup>10</sup> S. Raniwala,<sup>10</sup> N. K. Rao,<sup>7</sup> F. Retiere,<sup>9</sup> K. Reygers,<sup>8</sup> G. Roland,<sup>12</sup> L. Rosselet,<sup>3</sup> I. Roufanov,<sup>5</sup> C. Roy,<sup>9</sup> J. M. Rubio,<sup>3</sup> S. S. Sambyal,<sup>7</sup> R. Santo,<sup>8</sup> S. Sato,<sup>14</sup> H. Schlagheck,<sup>8</sup> H.-R. Schmidt,<sup>17</sup> Y. Schutz,<sup>9</sup> G. Shabratova,<sup>5</sup> T. H. Shah,<sup>7</sup> I. Sibiriak,<sup>4</sup> T. Siemiarczuk,<sup>19</sup> D. Silvermyr,<sup>11</sup> B. C. Sinha,<sup>2</sup> N. Slavine,<sup>5</sup> K. Söderström,<sup>11</sup> G. Sood,<sup>1</sup> S. P. Sørensen,<sup>20</sup> P. Stankus,<sup>6</sup> G. Stefanek,<sup>19</sup> P. Steinberg,<sup>12</sup> E. Stenlund,<sup>11</sup> M. Sumera,<sup>18</sup> T. Svensson,<sup>11</sup> A. Tsvetkov,<sup>4</sup> L. Tykarski,<sup>19</sup> E. C. v.d. Pijll,<sup>15</sup> N. v. Eijndhoven,<sup>15</sup> G. J. v. Nieuwenhuizen,<sup>12</sup> A. Vinogradov,<sup>4</sup> Y. P. Viyogi,<sup>2</sup> A. Vodopianov,<sup>5</sup> S. Vörös,<sup>3</sup> B. Wyslouch,<sup>12</sup> and G. R. Young<sup>6</sup>

(WA98 Collaboration)

<sup>1</sup>University of Panjab, Chandigarh 160014, India

<sup>2</sup>Variable Energy Cyclotron Centre, Calcutta 700064, India

<sup>3</sup>University of Geneva, CH-1211, Geneva 4, Switzerland

<sup>4</sup>RRC “Kurchatov Institute”, RU-123182, Moscow

<sup>5</sup>Joint Institute for Nuclear Research, RU-141980 Dubna, Russia

<sup>6</sup>Oak Ridge National Laboratory, Oak Ridge, Tennessee 37831-6372, USA

<sup>7</sup>University of Jammu, Jammu 180001, India

<sup>8</sup>University of Münster, D-48149 Münster, Germany

<sup>9</sup>SUBATECH, Ecole des Mines, Nantes, France

<sup>10</sup>University of Rajasthan, Jaipur 302004, Rajasthan, India

<sup>11</sup>University of Lund, SE-221 00 Lund, Sweden

<sup>12</sup>MIT, Cambridge, Massachusetts 02139, USA

<sup>13</sup>Institute of Physics, Bhubaneswar 751005, India

<sup>14</sup>University of Tsukuba, Ibaraki 305, Japan

<sup>15</sup>Universiteit Utrecht/NIKHEF, NL-3508 TA Utrecht, The Netherlands

<sup>16</sup>KVI, University of Groningen, NL-9747 AA Groningen, The Netherlands

<sup>17</sup>Gesellschaft für Schwerionenforschung (GSI), D-64220 Darmstadt, Germany

<sup>18</sup>Nuclear Physics Institute, CZ-250 68 Rez, Czech Republic

<sup>19</sup>Institute for Nuclear Studies, 00-681 Warsaw, Poland

<sup>20</sup>University of Tennessee, Knoxville, Tennessee 37966, USA

(Received 22 October 2003; published 6 July 2004)

Two-particle correlations of direct photons were measured in central  $^{208}\text{Pb} + ^{208}\text{Pb}$  collisions at 158A GeV. The invariant interferometric radii were extracted for  $100 < K_T < 300$  MeV/c and compared to radii extracted from charged pion correlations. The yield of soft direct photons,  $K_T < 300$  MeV/c, was extracted from the correlation strength and compared to theoretical calculations.

DOI: 10.1103/PhysRevLett.93.022301

PACS numbers: 25.75.Gz

Hanbury Brown–Twiss (HBT) interferometry provides a powerful tool to explore the space-time dimensions of the emitting source created in elementary particle or heavy ion collisions. Historically, such measurements have concentrated on pion pair correlations, but have

also been applied to kaons, protons, and even heavy fragments [1]. Hadron correlations reflect the space-time extent of the emitting source at the time of freeze-out.

The importance of direct photon Bose-Einstein interferometry for investigation of the history of heavy ion

collisions, especially of the very early phase, has been extensively discussed in the literature [2–6]. It has been shown that photon-photon correlations can provide information about the space-time distribution of the hot matter prior to freeze-out. Moreover, the correlations of direct photons of different transverse momenta will reflect different stages of the collision. Unfortunately, photon interferometry is faced with considerable difficulties compared to hadron interferometry primarily due to the small yield of photons emitted directly from the hot zone in comparison to the huge background of photons produced by the electromagnetic decay of the final hadrons ( $\pi^0$ 's). For this reason, there has been only one experimental measurement of photon-photon correlations in heavy ion collisions obtained at low incident energy and low photon momenta ( $K_T \leq 20$  MeV/c) [7]. In this Letter, we present first measurements of direct photon correlations in central ultrarelativistic heavy-ion collisions.

A detailed description of the layout of the CERN experiment WA98 can be found in [8]. Here we briefly discuss those subsystems used in the present analysis. The WA98 photon spectrometer, comprising the LEad-glass photon Detector Array (LEDA), was located at a distance of 21.5 m downstream from the  $^{208}\text{Pb}$  target. It provided partial azimuthal coverage over the rapidity interval  $2.35 < y < 2.95$ . Further downstream, the total transverse energy was measured in the MIRAC calorimeter. The total transverse energy measured in MIRAC was used for offline centrality selection. The analysis was performed on data collected in 1995 and 1996 for the 10% most central and 20% most peripheral fractions of the  $^{208}\text{Pb} + ^{208}\text{Pb}$  minimum bias cross section with total data samples of  $5.8 \times 10^6$  and  $3.9 \times 10^6$  events, respectively. No significant signal was observed in the peripheral data sample, consistent with the absence of any significant direct photon signal reported in [8].

In order to reject most of the hadron background, all showers reconstructed in the LEDA spectrometer were required to have a deposited energy of greater than 750 MeV, well above the minimum ionizing peak energy of 550 MeV. Hadron showers could be further rejected by the requirement that the shower have a narrow width, consistent with an electromagnetic shower in LEDA [8]. In addition, during the 1996 run period, the LEDA charged particle veto was operational and provided a shower sample of  $> 98\%$  photon purity.

The two-photon correlation function was calculated for each bin of the photon average transverse momentum,  $K_T = |\vec{p}_{T_1} + \vec{p}_{T_2}|/2$  as the ratio of the distribution of photon pair invariant relative momenta,  $Q_{\text{inv}}$ , where both photons were taken from the same event, to the same distribution but with the photons of the pair taken from different events. Sample correlation functions are shown in Fig. 1. The ratio was normalized to have an equal number of pairs in the numerator and denominator.

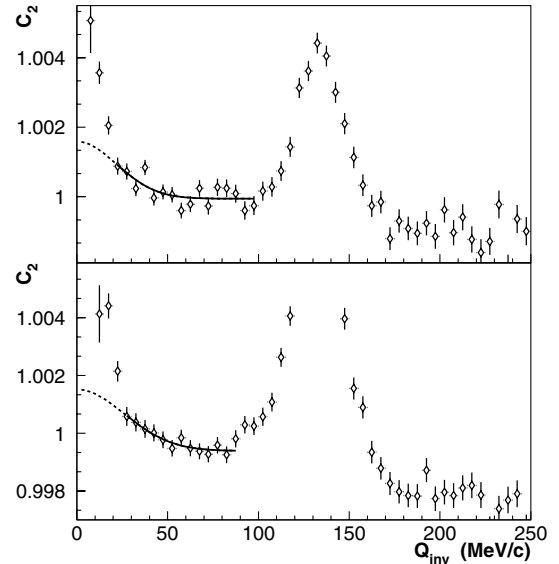


FIG. 1. The two-photon correlation function for narrow showers with  $L_{\text{min}} > 20$  cm (diamonds) and average photon momenta  $100 < K_T < 200$  MeV/c (top) and  $200 < K_T < 300$  MeV/c (bottom) fitted with Eq. (1). The solid line shows the fit result in the fit region used (excluding the  $\pi^0$  peak at  $Q_{\text{inv}} \approx m_{\pi^0}$ ) and the dotted line shows the extrapolation into the low  $Q_{\text{inv}}$  region where backgrounds are large.

The correlation function has been fit with a Gaussian parameterization with normalization  $A$ , correlation strength  $\lambda_{\text{inv}}$ , and radius parameter  $R_{\text{inv}}$ :

$$C_2(Q_{\text{inv}}) = A[1 + \lambda_{\text{inv}} \exp(-R_{\text{inv}}^2 Q_{\text{inv}}^2)]. \quad (1)$$

There are a large number of effects which may give rise to small  $Q_{\text{inv}}$  correlations and mimic a direct photon Bose-Einstein correlation. These include (i) single hadron or photon showers that are split into nearby clusters, (ii) photon conversions, (iii) HBT correlations of charged pions or other hadrons misidentified as photons, (iv) residual photon correlations from  $\pi^0$  HBT correlations, (v) radiative decays of heavier resonances, and (vi) collective flow.

Apparatus or analysis effects which may result in the splitting of a single shower into multiple clusters, or the merging of nearby showers into a single cluster, may be investigated by studying the dependence of the correlation function on the relative distance  $L$  between the showers on the LEDA detector surface. These effects are expected to contribute strongly at small  $L$  and so can be suppressed effectively by a distance cut. Such a minimum cut on  $L$  introduces a lower cutoff in  $Q_{\text{inv}}$  [9].

The dependence of the correlation strength parameter  $\lambda_{\text{inv}}$  on the minimum distance cut  $L_{\text{min}}$  and the minimum invariant momentum  $Q_{\text{min}}$  used to define the fit region is shown in Fig. 2 for two  $K_T$  regions for narrow showers. The different symbols correspond to minimum distance cuts of  $L_{\text{min}} = 20, 25, 30,$  and  $35$  cm (note that a single

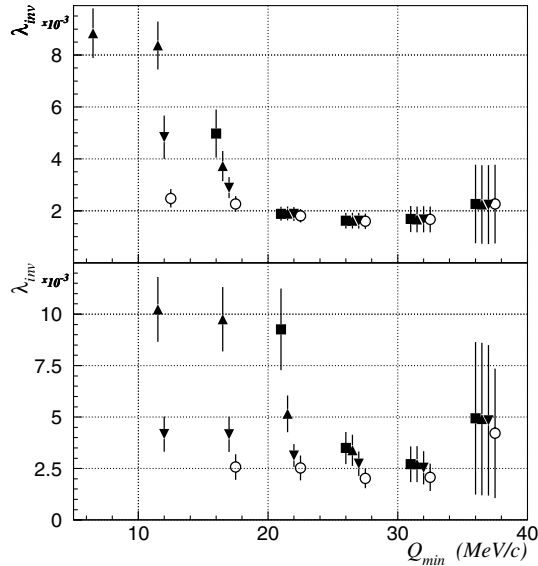


FIG. 2. Comparison of  $\lambda_{inv}$  parameter fit results for different fit regions for  $100 < K_T < 200$  MeV/c (top) and  $200 < K_T < 300$  MeV/c (bottom), calculated for narrow showers with different cuts on the minimum shower separation distance:  $L_{min} = 20$  cm,  $\blacksquare$ ; 25 cm,  $\blacktriangle$ ; 30 cm,  $\blacktriangledown$ ; 35 cm,  $\circ$  (same  $Q_{min}$  for each).

LEDA module is 4 cm in width). The results demonstrate that the extracted fit parameters vary strongly with  $L_{min}$  when the low  $Q_{inv}$  region is included in the fit, a result attributed to apparatus effects and conversion background, but that stable results are obtained with a sufficiently large minimum separation distance cut, or by restricting the  $Q_{inv}$  fit region. When no charged veto or narrow shape cuts are applied to the showers, stable results are also obtained, but with larger minimum distance cut (or  $Q_{min}$ ) required, consistent with the larger expected backgrounds.

As mentioned above, the observed correlations could be caused by residual correlations of charged pions, neutrons, antineutrons, or conversion electrons misidentified as photons. To investigate possible contributions from nonphoton contamination, the correlation functions were constructed with four different identification criteria applied to the showers reconstructed in LEDA. These criteria have somewhat different photon efficiencies, which should not affect the photon correlation, but more importantly have very different levels of nonphoton contamination which should only affect  $\lambda_{inv}$  if the contamination forms uncorrelated background. The charged hadron contamination decreases from 37% and 22% to 16% and 4%, respectively, for the two  $K_T$  bins, after applying the narrow electromagnetic shower shape condition [8] and is negligible after application of the charged veto condition. The correlation parameters extracted from these four types of correlation functions, corrected for contamination, are shown in Fig. 3. The

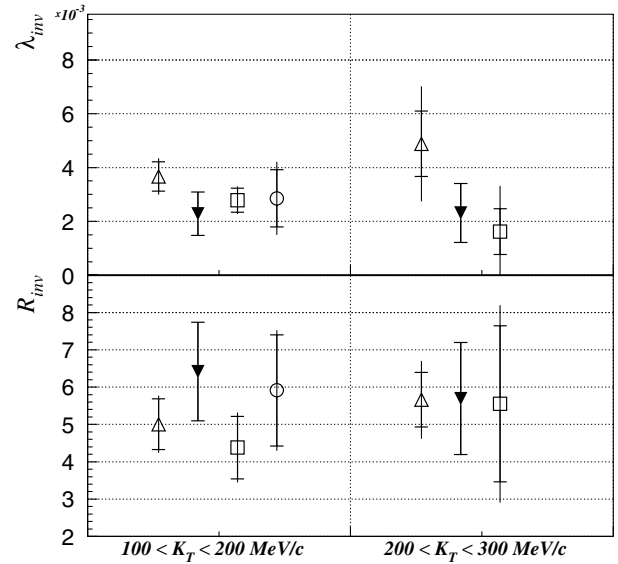


FIG. 3. Comparison of parameters of correlation functions with different particle identification criteria:  $\Delta$ , all clusters;  $\blacktriangledown$ , narrow electromagnetic;  $\square$ , all neutral;  $\circ$ , narrow neutral electromagnetic (no significant result for high  $K_T$ ).

consistency of the parameters extracted with the different identification criteria indicates that the nonphoton contribution to the observed correlation is not significant.

The estimated systematic errors on the correlation fit parameters are summarized in Table I. Besides the uncertainties associated with the apparatus and fit range discussed with respect to Fig. 2, and nonphoton contamination (Fig. 3), the dependence on the fit function has been investigated. In addition to the Gaussian form of Eq. (1), an exponential form and a student's  $t$  distribution form have also been used to fit the correlation functions. The student's  $t$  distribution provides a good fit to the correlation for parameter  $n \geq 2$ . The variation of the fit results with  $n$  and comparison with the Gaussian fit results has been used to estimate the fit function error. Reasonable fit functions leading to significantly smaller values of  $\lambda_{inv}$  could not be found. An exponential form gives larger

TABLE I. Summary of relative systematic errors on the photon-photon correlation parameters (in %).

Source	$100 < K_T < 200$		$200 < K_T < 300$	
	$\lambda_{inv}$	$R_{inv}$	$\lambda_{inv}$	$R_{inv}$
Apparatus	7	5	16	6
Contamination	17	14	42	14
Fit function	5	5	18	6
Fit range	8	5	26	10
$Q_{inv}$ slope (flow + BE)	2	3	12	8
Total systematic error (%)	21	17	56	21
$N_{\gamma}^{total}$ total error (%)	12	...	4	...

$\lambda_{\text{inv}}$  values but also exhibits a strong dependence of the fit parameters on fit range.

Finally, correlations might exist in the background decay photons, e.g., correlations due to collective flow, Bose-Einstein correlations of  $\pi^0$ 's, or from decays of heavier resonances. Monte Carlo simulations have been performed to estimate each of these effects. For these simulations, the transverse momentum and rapidity distributions of the  $\pi^0$ 's were taken from measurements [8]. The effect of flow was investigated by introducing an elliptic flow pattern with a magnitude equal to that measured for charged pions [10]. Similarly, the effect of  $\pi^0$  Bose-Einstein correlations was introduced with the same parameters as measured for charged pions [11]. Finally, residual correlations due to decays of heavier resonances were estimated by including all resonances having high yield and large branching ratios for electromagnetic decay:  $K_S^0$ ,  $K_L^0$ ,  $\eta$ , and  $\omega$ . The heavy resonances were included based on experimental spectra where available and thermodynamic extrapolations otherwise. In all simulations, the acceptance, identification cuts, and energy and position resolution of LEDA were applied. The simulations showed that elliptic flow results in the

appearance of a small slope in the correlation function and that Bose-Einstein correlations of  $\pi^0$ 's lead to a characteristic steplike structure in the photon-pair correlation function at the  $\pi^0$  mass, with a small slope in the  $Q_{\text{inv}} < 100$  MeV/c region, also shown by analytical calculations [5]. The height of the step in simulations agrees with that seen in the correlation functions of Fig. 1. The contribution of residual correlations due to decays of heavier resonances results in a deviation from unity which is smaller than  $10^{-4}$ . The combination of these effects in simulation results in a predicted slope in the photon-pair correlation of  $5 \times 10^{-6}$  (MeV/c) $^{-1}$  in the region of fit. The data sample with the highest statistics has been fit with an additional parameter for the slope, and the extracted value of  $(5 \pm 3) \times 10^{-6}$  (MeV/c) $^{-1}$  was found to be consistent with the simulation result. However, limited statistics did not allow to extract a slope value for all data samples. Therefore, the final values of the correlation strength and radii have been corrected for the presence of an overall slope using the simulation result (typically a 10% decrease of  $\lambda_{\text{inv}}$  and 10% increase of  $R_{\text{inv}}$ ).

Averaging over the different particle identification criteria, we obtain the following correlation parameters:

$$\begin{aligned} \lambda_{\text{inv}}^{\text{I}} &= 0.0028 \pm 0.0004(\text{stat}) \pm 0.0006(\text{syst}), & R_{\text{inv}}^{\text{I}} &= 5.9 \pm 0.8(\text{stat}) \pm 0.9(\text{syst}) \text{ fm}, \\ \lambda_{\text{inv}}^{\text{II}} &= 0.0029 \pm 0.0007(\text{stat}) \pm 0.0016(\text{syst}), & R_{\text{inv}}^{\text{II}} &= 6.1 \pm 0.8(\text{stat}) \pm 1.2(\text{syst}) \text{ fm}, \end{aligned}$$

for regions (I)  $100 < K_T < 200$  MeV/c and (II)  $200 < K_T < 300$  MeV/c, respectively.

The correlation function can be written as an integral over directions of the relative momenta in the pair c.m. frame. For massless particles it can be expressed as

$$C_2(Q_{\text{inv}}, K_T) = 1 + \frac{\lambda}{4\pi} \int d\Omega \exp\{-(Q_{\text{inv}}^2 + 4K_T^2)R_O^2 \cos^2\theta - Q_{\text{inv}}^2(R_S^2 \sin^2\theta \sin^2\phi + R_L^2 \sin^2\theta \cos^2\phi)\},$$

where  $\lambda$  is the correlation strength ( $\lambda = 1/2$  for a fully chaotic photon source),  $R_O$ ,  $R_S$ , and  $R_L$  are the ‘‘out’’ ‘‘side,’’ and ‘‘long’’ radius components of the source, measured in the local comover system. For large  $K_T$  ( $\gg Q_{\text{inv}}$ ), the photon  $R_{\text{inv}}$  is an average of  $R_S$  and  $R_L$ , and almost independent of  $R_O$ . However, the measured invariant correlation strength is dependent on  $R_O$  as  $\lambda_{\text{inv}} = \lambda \times \sqrt{\pi} \text{Erf}(2K_T R_O) / 4K_T R_O$ . Therefore the direct photon invariant radii may be compared to measurements of the side and long components of interferometric radii of  $\pi^-$  for the same centrality selection and similar  $K_T$  region [12]:  $R_S = 5.55 \pm 0.24$ ,  $5.13 \pm 0.32$ , and  $4.81 \pm 0.29$  fm,  $R_L = 5.95 \pm 0.27$ ,  $5.45 \pm 0.37$ , and  $5.15 \pm 0.34$  at  $K_T = 125$ ,  $175$ , and  $285$  MeV/c, respectively. The similarity of the interferometric radii of direct photons and pions suggests that the direct photons of this  $K_T$  region are emitted in the late stage of the collision.

Under the assumption of a fully chaotic photon source, the direct photon yield  $N_\gamma^{\text{direct}}$  is related to the correlation strength  $\lambda$  and the total inclusive photon yield  $N_\gamma^{\text{total}}$  as [5]

$$N_\gamma^{\text{direct}} / N_\gamma^{\text{total}} = \sqrt{2\lambda} = \sqrt{8\lambda_{\text{inv}} K_T R_O / \sqrt{\pi} \text{Erf}(2K_T R_O)}.$$

Although the photon  $R_O$  has not been measured, a *lower* limit on the yield of direct photons is given by the assumption  $R_O = 0$ . A *most probable* yield is obtained by assuming a value of  $R_O = 6$  fm [12]. The low  $p_T$  direct photon yields have been extracted for these two cases and are presented in Fig. 4 (assuming  $p_T = \langle K_T \rangle$ ). The previously published direct photon yield at high transverse momenta obtained with the subtraction method [8] is also shown. The measured direct photon results are compared with recent fireball model predictions [13]. The calculated contributions to the total yield from the quark gluon plasma and hadronic stages of the collision are shown. It is seen that the contribution from the hadron gas phase dominates the direct photon yield at small  $p_T$ , with predicted yields below the measured direct photon yield.

In summary, two-photon correlation functions have been measured for the first time in central

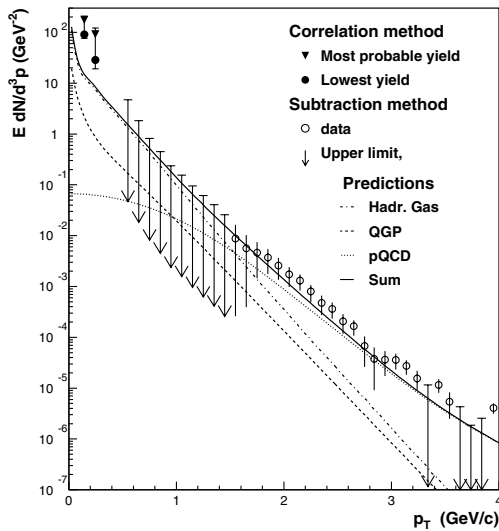


FIG. 4. Yield of direct photons extracted from the strength of the two-photon correlation ( $R_O = 0$  fm, closed circles;  $R_O = 6$  fm, closed triangles) and by the statistical subtraction method (open circles, or arrows indicating upper limits) [8]. Total statistical plus systematical errors are shown. The calculations are described in the text.

$^{208}\text{Pb} + ^{208}\text{Pb}$  collisions at 158A GeV. The observed correlations are attributed to Bose-Einstein correlations of directly radiated photons. An invariant photon source radius of about 6 fm is extracted at low momenta, comparable to correlation radii extracted for pions of similar momenta. The correlation strength parameter was used to determine the yield of direct photons at  $p_T < 300$  MeV/c. The measured yield exceeds theoretical expectations which attribute the dominant contribution in this  $p_T$  region to the hadronic phase.

We wish to acknowledge useful discussions with R. Rapp, C. Gale, and D. Srivastava. This work was supported jointly by Russian NS-1885.2003.2, the German BMBF and DFG, the U.S. DOE, the Swedish NFR and FRN, the Dutch Stichting FOM, the Polish KBN under Contract No. 621/E-78/SPUB-M/CERN/P-03/DZ211/, the Grant Agency of the Czech Republic under Contract No. 202/95/0217, the Department of

Atomic Energy, the Department of Science and Technology, the Council of Scientific and Industrial Research and the University Grants Commission of the Government of India, the Indo-FRG Exchange Program, the PPE division of CERN, the Swiss National Fund, the INTAS under Contract No. INTAS-97-0158, ORISE, Grant-in-Aid for Scientific Research (Specially Promoted Research & International Scientific Research) of the Ministry of Education, Science and Culture, the University of Tsukuba Special Research Projects, and the JSPS. ORNL is managed by UT-Battelle, LLC, for the U.S. Department of Energy under Contract No. DE-AC05-00OR22725. The MIT group has been supported by the U.S. Department of Energy under the cooperative agreement DE-FC02-94ER40818.

\*Deceased.

- [1] See, e.g., W. Bauer, C. K. Gelbke, and S. Pratt, *Annu. Rev. Nucl. Part. Sci.* **42**, 77 (1992); U. Heinz and B. Jacak, *Annu. Rev. Nucl. Part. Sci.* **49**, 529 (1999).
- [2] D. K. Srivastava and J. I. Kapusta, *Phys. Lett. B* **307**, 1 (1993); *Phys. Rev. C* **48**, 1335 (1993); *Phys. Rev. C* **50**, 505 (1994).
- [3] A. Timmermann, M. Plumer, L. Razumov, and R. M. Weiner, *Phys. Rev. C* **50**, 3060 (1994).
- [4] U. Ornik *et al.*, hep-ph/9509367.
- [5] D. Peressounko, *Phys. Rev. C* **67**, 014905 (2003).
- [6] J. Alam, B. Mohanty, P. Roy, S. Sarkar, and B. Sinha, *Phys. Rev. C* **67**, 054902 (2003).
- [7] M. Marques *et al.*, *Phys. Rep.* **284**, 91(1997); *Phys. Rev. Lett.* **73**, 34 (1994); *Phys. Lett. B* **349**, 30 (1995).
- [8] M. M. Aggarwal *et al.*, *Phys. Rev. Lett.* **85**, 3595 (2000); M. M. Aggarwal *et al.*, nucl-ex/0006007.
- [9] Since  $Q_{\text{inv}}$  is proportional to  $K_T$ , the distance cut implies that the low  $Q_{\text{inv}}$  Bose-Einstein enhancement of the correlation is observable here only at low  $K_T$ .
- [10] H. Appelshauser *et al.*, *Phys. Rev. Lett.* **80**, 4136 (1998).
- [11] K. Kadija *et al.*, *Nucl. Phys. A* **610**, 248c (1996).
- [12] M. M. Aggarwal *et al.*, *Phys. Rev. C* **67**, 014906 (2003).
- [13] S. Turbide, R. Rapp, and C. Gale, *Phys. Rev. C* **69**, 014903 (2004).